Nanoscale

Redox processes at a nanostructured interface under strong electric fields

Journal:	*Nanoscale*
Manuscript ID:	NR-ART-05-2014-002882
Article Type:	Paper
Date Submitted by the Author:	26-May-2014

Complete List of Authors:	Steurer, Wolfram; IBM Research GmbH, Surnev, S; Karl-Franzens-Universität Graz, Netzer, Falko; Institute of Experimental Physics, Surface and Interface Physics Division; Karl-Franzens-Universität Graz, Sementa, Luca; Consiglio Nazionale delle Ricerche (CNR), Istituto per i Processi Chimico-Fisici (IPCF-CNR) Negreiros, Fabio; Consiglio Nazionale delle Ricerche (CNR), Istituto per i Processi Chimico-Fisici (IPCF-CNR) Barcaro, Giovanni; Consiglio Nazionale delle Ricerche (CNR), Instituto per i Processi Chimico-Fisici (IPCF-CNR) Durante, Nicola; Consiglio Nazionale delle Ricerche (CNR), Instituto per i Processi Chimico-Fisici (IPCF-CNR) Fortunelli, Alessandro; CNR,

Redox processes at a nanostructured interface under strong electric fields

Wolfram Steurer, Svetlozar Surnev, Falko P. Netzer
Surface and Interface Physics, Institute of Physics, Karl-Franzens University Graz, A-8010 Graz, Austria

Luca Sementa, Fabio R. Negreiros, Giovanni Barcaro, Nicola Durante, Alessandro Fortunelli
CNR-ICCOM & IPCF, Consiglio Nazionale delle Ricerche, I-56124 Pisa, Italy

Abstract

Manipulation of chemistry and film growth via external electric fields is a longstanding goal in surface science. Numerous systems have been predicted to show such effects but experimental evidence is sparse. Here we demonstrate in a custom-designed UHV apparatus that the application of spatially-extended, homogeneous, very high (> 1 V/nm) DC-fields not only changes the system energetics but triggers dynamic processes which become important much before static contributions appreciably modify the potential energy landscape. We take a well characterized ultrathin NiO film on a Ag(100) support as a proof-of-principle test case, and show how it gets reduced to supported Ni clusters under fields exceeding the threshold of +0.9 V/nm. Using an effective model, we trace the observed interfacial redox process down to a dissociative electron attachment resonant mechanism. The proposed approach can be easily implemented and generally applied to a wide range of interfacial systems, thus opening new opportunities for the manipulation of film growth and reaction processes at solid surfaces under strong external fields.

The ability to control redox processes such as selective excitation and dissociation of bonds through the manipulation of electron interactions[1] is one of the great challenges of modern research, representing one main path to the transformation of physical into chemical energy, which is believed to be crucial for future energy storage.[2] Several routes have been explored in this context, ranging from plasma treatment in the gas-phase to electron bombardment or photoemission from a conducting substrate for species deposited on surfaces,[3,4] and research is currently focused on how to achieve the efficiency and atom selectivity required for real-world applications.

A different tool which is being concurrently investigated in both advanced research and technology [5,6,7] to achieve selective processes is tuning the system energetics via applied external fields. For example, electric fields can be used to orient atomic surface arrangements with the perspective of creating novel structures with properties tailored to specific applications[8] or be exploited at the dynamic level to promote and trigger electrochemical reactions in solution[9] or in heterogeneous catalysis.[10]

In the present work, we propose a novel method which combines features of both these approaches: we realize a surface-science ultra-high vacuum (UHV) apparatus in which very high electric field gradients can be achieved, and demonstrate via experimental analysis and theoretical modeling that the application of a spatially-extended homogeneous electric field simultaneously affects the system energetics and induces a controlled electron flow, which in turn gives rise to an interfacial redox process exhibiting resonance features. We illustrate the method in the specific case of a nickel oxide (2x1) ultra-thin film grown on Ag(100), chosen for its being a fully characterized and spatially homogeneous polar oxide phase,[11,12] by showing its reduction to supported Ni clusters when a DC-field exceeding the threshold of +0.9 V/nm is turned on, but the approach is general and can be applied to a wide range of interfacial systems – the subject of future investigations.

Despite numerous theoretical predictions,[13,14,15,16,17,18,19,20] experiments demonstrating the influence of strong homogenous external electric fields on surface processes are rare. The experiments here described were performed in a custom-designed UHV system (base pressure $1x10^{-10}$ mbar) with facilities for sample cleaning and thin-film preparation, an in-house constructed setup for applying external DC-fields, and surface characterization techniques including low-energy electron diffraction (LEED), scanning tunneling microscopy (Omicron VT-STM), and Auger electron spectroscopy (AES). The E-field set-up is described in detail in Ref.[21] and is pictorially shown in Fig. 1. In brief, the miniature electrode is made out of quartz (SiO_2) with a gold film (3x5 mm^2) evaporated onto the

middle part, which is entrenched into the main body of the electrode by 800 nm with respect to the outer rims, which act as support legs. The miniature electrode is lowered from above onto the sample surface, which is inserted into the E-field stage with integrated sample heating. After landing on the sample, the miniature electrode stands force-free on the sample surface, thus ensuring a uniform gap of ~800 nm in between the gold coating of the electrode and the sample surface.

The Ag(100) substrate was cleaned by repeated cycles of Ar^+ sputtering (1 kV, 15μA/cm^2) and annealing at 700 K; order and cleanliness of the substrate were checked using LEED, AES and STM. Ultrathin NiO films were prepared by reactive deposition of 0.7 monolayers of Ni (as referenced to the atom density of the Ag(100) surface) in an oxygen atmosphere of $1x10^{-6}$ mbar. Routinely, the surface preparation was checked by LEED and STM before exposure to the electric field. As-prepared NiO/Ag(100) surfaces were post-annealed in the presence/absence of an electric field (-2 to 2 V/nm). Typically, the sample was annealed at 400 K for 20 min; in cases where an electric field was applied, the bias voltage was switched off after the sample had cooled down to below 330 K.

STM images of NiO/Ag(100) surfaces as deposited, and after annealing in the presence/absence of homogeneous DC-fields, are shown in Fig. 2. After reactive deposition at room temperature, a polar NiO (2x1) phase (green colored contrast) forms as evidenced by the appearance of adjacent bright and dark rows in the STM image. The surface morphology is characterized by small domains of only moderate order and two Ag height levels (yellow and dark contrast), which are separated by a random pattern of step edges (Fig. 2a). The (2x1) structures are embedded into the Ag substrate rather than being accommodated on top of the silver surface,[11] and consist of a polar stacking of Ni and O layers as described below.

In the absence of an electric field or for $\vec{E} < 0.9$ V/nm, annealing of the Ni-oxide covered surface at 400 K (either in vacuum or in oxygen) gives rise to well-ordered, single-phase (2x1) structures (green) embedded into the Ag substrate (yellow), as depicted in Fig. 2b (no field was applied in the case shown). Rectangular Ag islands with straight boundaries are observed. The stripes of the (2x1) phase, which arrange in domains rotated by 90° with respect to each other, are clearly discernible. A few vacancy islands are apparent, which are lowered by a single Ag step; they appear dark in the STM image. A number of defects are also seen in the NiO (2x1) areas, in particular close to the phase boundaries.

For positively polarized DC-fields exceeding the threshold of +0.9 V/nm, annealing of the as-deposited NiO/Ag(100) surface induces the formation of clusters (white contrast), which preferentially decorate the randomly-oriented boundaries of the small NiO (2x1) patches (green), as shown in Fig. 2c. An electric field of $\vec{E}$ = 1.5 V/nm was applied in this case. Interconnected Ag areas on two height levels are seen (yellow and dark green). Very similar surface morphologies (see Fig. 2d) are obtained if, instead of the as-deposited surface, the well-ordered NiO (2x1) surfaces like the one shown in Fig. 2b are *re*-annealed at $\vec{E}$ > 0.9 V/nm. In the case of Fig. 2d an electric field of $\vec{E}$ = 2.0 V/nm and an oxygen partial pressure ($1x10^{-7}$ mbar) were applied. A significant increase of the area fraction of bare Ag is revealed in Figs. 2c and 2d, which occurs at the expense of the Ni-oxide phase. Statistical analysis of the clusters reveals a mean diameter of 0.5±0.1 nm for Fig. 2c and 1.0±0.2 nm for Fig. 2d.

In order to elucidate the process causing the observed field-induced morphology changes, the field exposed and not-exposed surface areas have been analyzed by AES. This is readily possible, because the miniature electrode covers only a part of the substrate. Figure 3 presents AES data from the surface displayed in Fig. 2d (see SI[25] for an AES spectrum recorded on the surface shown in Fig. 2c). The red curve (I_F) has been recorded approximately at the position of the STM image, the black curve (I_0) at a location not covered by the miniature electrode, which exhibited thus the surface morphology as in Fig. 2b. The difference $(I_0-I_F)/max(I_0)$ of the two AES curves is plotted at the bottom of Fig. 3 [dots – point-by-point ratio, red line – moving-window average (8 points)]. Significant deviations from zero are only observed around 350 eV ($I_F>I_0$) and 500 eV ($I_F<I_0$). An enlarged view of the energy window 450÷550 eV, measured with higher sensitivity, is presented in the inset of Fig. 3. A decrease of the oxygen content by a factor of two between exposed and not-exposed surface areas is revealed. The solid lines are moving-window averages and serve as a guide to the eye.

We interpret the observed field-induced changes as a partial reduction of the initial Ni-oxide film. For field strengths exceeding the threshold of 0.9±0.2 V/nm, oxygen atoms are removed from the surface: the Auger spectra in Fig. 3 reveal a clear reduction of the oxygen KLL peaks on field-exposed areas. The remaining Ni atoms are highly mobile on the Ag surface and cluster together, as in experiments on epitaxial growth of Ni on Ag(100).[22] Note that electron bombardment upon impingement is not effective in our case as the reduction phenomenon is *only* observed for *positive* field polarities (field-emitted electrons leaving the Ag substrate). The bombardment of the Au electrode at positive field

polarities could potentially cause Au contamination of the sample surface. However, this possibility is ruled out by the AES spectra presented in the SI[25], which do not feature an additional peak at around 85 eV or other contamination peaks.

At the high field strengths applied, electrons are emitted everywhere on the cathode surface, in principle homogeneously on an ideal cathode surface. In practice, however, a perfectly smooth surface does not exist and the largest fraction of electrons is emitted from a small number of so-called "hot spots", i. e., sharp-pointed defects like spikes or small grains.[23] In fact, the emission area, as well as the contribution of these hot spots to the total emission current, can be estimated from Fowler-Nordheim I-V curves[24] (see Supplementary Information, SI[25]). For the experiments shown here, the total emission current fluctuated between 50 and 100 μA; analysis of Fowler-Nordheim I-V curves yields values between 10^3 and 10^5 nm^2 for the area of the hot spots and 0.8÷0.9 for their contribution to the total emission current, respectively. Assuming that the emission of electrons is homogeneous on the remaining areas of the electrode, a lower limit for the efficiency of the reduction process can be estimated by dividing the number of reduced NiO species by the total number of emitted electrons, disregarding the ones emitted by the hot spots. It results an efficiency of $\approx 2.5\ 10^{-3}$ for the reduction process (see SI[25]). Note that we have routinely recorded STM images on different locations on the sample that were exposed to the field[a] without observing notable differences. Only in two or three occasions we happened to image surface regions that looked markedly different from Figs. 2(c,d). These areas displayed much larger clusters and showed a high degree of surface anisotropy, indicative of exposure to an inhomogeneous electric field as it will occur in the proximity of surface asperities or "hot spots". An example of such a surface area is shown in the SI[25].

Theoretical modeling of the present experiment is not a routine task. Strong electric fields are treated in most current theoretical simulations within the framework of static perturbation theory.[13,14,15,16,17,18,19,20] Although this level of modeling can be qualitatively suggestive, the physics which actually occurs is as a norm quite different. One often finds in fact that at the static level very large values of the field – of the order of 20-50 V/nm – are required to obtain an appreciable effect on the system static potential energy surface (PES), and indeed we performed extensive DFT calculations showing that this is also the case for the present NiO/Ag(100)-(2x1) phase.[26] Such values are unrealistic, being one order of magnitude larger than the maximum values experimentally accessible (around 1-3 V/nm). For example

[a] The field-exposed area is readily located by eye because of its macroscopic dimension of 3x5 mm^2.

in our experiments for fields larger than 2-3 V/nm even in the case of a perfectly smooth electrode surface the field emission current of electrons leaving the cathode exceeds reasonable values (<500 mA) and causes a rapid destruction of the electrode. In real systems, thus, much before values of electric field as high as 20-50 V/nm are reached, dynamic processes start being activated, basically related to non-equilibrium electron tunneling and transport.[27,28] In the present case we argue that dissociative electron attachment (DEA)[29,30] is effective, i.e., a resonant process occurring at low electron energies and characterized by the initial capture of an electron to form a transient negative ion that subsequently gives rise to dissociation, so that an oxygen atom detaches as an O^- anion from the NiO phase.[31] Negative ion resonances manifest themselves in a wide range of experimental conditions, from electron/molecule scattering to surface photochemistry, including the case of interfacial systems or DEA at surfaces, 3,4,[32,33,34,35,36] and a common physics basically underpins these phenomena.

The complexity of the problem: non-equilibrium electron transport[37] in an extended interfacial (multi-component) system – whose atomistic arrangement is schematically shown in Fig. 4(a) – precludes a fully quantitative theoretical treatment. Rather, we build upon the theory of electron/diatomic-molecule DEA[29,32,3,33,34,4,35,36] and reproduce the salient features of the phenomenon by mapping our poly-atomic system onto a one-dimensional (1-D) effective model exhibiting only a bound and a dissociative state. Two ingredients are necessary to this purpose: the electronic capture matrix element and the potential energy surfaces as a function of the 1-D geometry. With respect to previous literature, the matrix element of the electron capture process is evaluated in a slightly different way. Concentrating attention on an outermost NiO pair, which is the most prone to oxygen detachment for geometric and energetic reasons, the extended NiO/Ag(100)-(2x1) phase is simplified and replaced by a diatomic A-B molecule outside a metal surface (A stands for the nickel and B for the oxygen atom), see Fig. 4(b). Moreover we utilize a minimal representation of active electrons, replace the electron/nucleus attractive Coulomb potentials with Dirac delta-functions[38] (see SI[25]), and solve the problem in one-dimension (the *x*-axis) which is the direction of electron scattering, see Fig. 4(c). The solutions for the electronic wave functions in terms of localized and continuum orbitals are schematically shown in Fig. 4(c).[25] In particular, one finds a ground state orbital $\phi_b(x)$ with energy $\varepsilon_b(R)$ (R is the interatomic distance) and one can construct a localized resonance state responsible for electronic capture[29] as an anti-bonding orbital $\phi_a(x)$ with energy $\varepsilon_a(R)$. The continuum orbitals corresponding to incoming waves with electronic momentum k and kinetic electronic energy: $\varepsilon_k = k^2/2$ are denoted as $\phi_k(x)$. These orbitals are orthogonal to $\phi_b(x)$ by construction, and are Schmidt-orthogonalized to $\phi_a(x)$. The matrix element of the electronic capture process, ECP(k; R), as a function of k and R is then calculated as:

$$ECP(k; R) = \int dx\, \phi_a(x)\, \hat{H}_{el}\, \phi_k(x) \quad (1)$$

where $\hat{H}_{el}$ is the electronic Hamiltonian, sum of nuclear attraction and the electronic kinetic energy. As the parameters of the delta-function model are extracted by an analysis of DFT calculations on the real system (see SI[25]), we trust that the evaluation of electronic capture matrix element is accurate.

In setting up the nuclear Hamiltonian, i.e., the $PES_i(R)$ and $PES_f(R)$ on which the nuclei of the AB and AB^- species move, respectively, the following factors should in principle be taken into account: (i) Intersystem crossing among several (actually, very many) PES – the electronic bands occupied at equilibrium in the NiO/Ag(100)-(2x1) phase evolve in a complex way as periodic symmetry is broken, an oxygen atom detaches, and its atomic orbitals disentangle from the band envelope (this is analogous – only, even more complex – to surface hopping in atom/surface collisions);[39] (ii) Image-charge interactions – due to the polarization of the Ag(100) support, the electric field generated by charge-separated species such as ions or dipoles produces a stabilizing image-charge response which holds also for the travelling electron once it is localized on the oxygen atom as far as retardation effects can be neglected; (iii) Electric field – the external electric field is not only the source of electron current but also deforms the nuclear PES: a value of 1 V/nm corresponds to an energy drop of 1 eV over a distance of ≈20 a.u., and even though this is not sufficient to explain the reduction process it does contribute to the system energetics. We approximately capture the interplay of these effects in our model set-up – see Fig. 4(c) – by deriving the energetics of the NiO/Ag(100)-(2x1) phase from DFT calculations (see SI[25] for more details) also including stabilizing electric-field and image-charge contributions, thus finally obtaining the PES reported in Fig. 5(a).[40] We then evaluate the nuclear wave functions (both the ground-state initial one on PES_i and the outgoing final one on PES_f at given values of nuclear energy $\eta = K^2/2$ in the AB^- continuum, where K is the nuclear momentum) and finally calculate the cross section of the DEA process as:

$$\Theta(\eta) = \left| \int dR\, GS_0(R) \cdot ECP(k; R) \cdot OC_1(\eta; R) \right|^2 \quad (2)$$

where $GS_0(R)$ is the ground-state AB nuclear wave function, $OC_1(\eta; R)$ is the outgoing final nuclear wave function at a given energy η in the continuum, and $ECP(k; R)$ is the matrix element of the electronic capture process from Eq. (1). The value of η is calculated by energy conservation as $\eta = E_i - EA(B)$, with E_i the total energy of the system in the initial configuration (an incoming electron with momentum k and the AB molecule in its electronic and vibrational ground state) and EA(B) the

electron affinity of the B atom: this corresponds to neglecting dissipation into the system's other degrees of freedom which lie outside our model (such as nuclear excitations via inelastic electron tunneling),[41] in addition the non-conservative character caused by the external field. A plot of $\Theta(\eta)$ for a value of $k^2/2$ equal to 2.0 eV is given in Fig. 5(b). Two features are apparent from an inspection of Fig. 5(b): (i) the probability of the capture and dissociation process within this simplified model possesses a clear resonant character (energy threshold or activated process), (ii) the corresponding DEA cross-section has a maximum at about $5x10^{-3}$, meaning that the efficiency of the process is estimated to be at the maximum around one reactive process (DEA reduction) each 200 electron tunneling events through a surface oxygen atom. Both these features are fully in tune with and provide a theoretical basis to experimental observations. It can be noted that in the real surface oxide the O atoms are two-fold coordinated and Ni-O is not a terminal group as in our simplified diatomic model, but – as in DEA in multi-atom system when more than one channel is operative [3,4] – we expect the total efficiency of the process to be close to the sum of the different channels. It should also be underlined that if the field polarity is inverted the incoming electron will still form a resonant anionic state, but the O anion will be pushed towards the surface and will not dissociate, so that reduction of our polar phase is predicted only for positively polarized DC fields.

In recent years studies of electric-field-induced effects have explored the influence of inhomogeneous electric fields as they occur in the proximity of the tips used in atomic force microscopy (AFM) and scanning tunneling microscopy (STM),[37,42,43,44,45,46,47] with the goal of understanding the influence of the tip during surface imaging or measuring kinetic surface properties like diffusion rates.[48] In this perspective our approach can be seen as the area-averaged analogue of tip- (or better tunneling-current-)promoted chemistry in STM experiments, with the advantageous complementarity of area-averaged with respect to local techniques. Indeed during STM scanning of the NiO/Ag(100) phase we observed frequent tip changes likely associated with mass transport (i.e., likely jumps of atoms from the surface to the tip) and the emergence of cluster-like features from one scan to the next, see SI[25]. The present electric-field experiment allows us to interpret these sudden tip changes as due to oxygen detachment from the NiO phase. In this connection it should be stressed that STM tip changes are observed *only* for negative biases *below* -1.2 V, in perfect tune with the resonant (threshold-limited) and selective (only positive field polarities) character of the DEA observed in the homogeneous-field apparatus. We believe that oxygen detachment from oxide ultrathin phases during STM measurements at sufficiently large negative biases is a very common phenomenon whose comprehension the present work achieves and puts on a rigorous basis.

Among non-equilibrium electron transport effects induced by strong electric fields another important phenomenon competing with DEA is current-promoted surface diffusion and mobility. In Ref.[5], an oxide/ionic-liquid resistive switching was considered, and it was shown that atoms/defects can be displaced at the interface by applying electric fields. Somewhat closer to the present work is Ref.8 in which electric-field-induced surface diffusion and nanoscale island growth on gold surfaces subjected to electric fields of the order of 0.1 to 1 V/nm have been reported. In general, this is connected with what might be called the system "horror cuspidis" in the presence of strong electric fields, i.e. the tendency to avoid and/or suppress surface structural asperities due to field and current enhancement at pointed tips. This is however different from the redox chemical processes reported here, and can occur in a different region of the parameter space. Indeed, we have experimental evidence that by switching from NiO/Ag(100)-(2x1) to the structurally homologous MnO/Ag(100)-(2x1) phase (i.e., simply changing Ni into Mn) a quite different physics (closer to what reported in Refs.[5,8]) takes place: current-induced Ag surface diffusion prevails over MnO DEA because the DEA threshold shifts to higher energies[49] and thus higher fields, but before these are reached Ag diffusion is activated with the corresponding formation of Ag clusters on top of the MnO(2x1) phase (this will be the subject of a future report).

In summary, here we explore a novel approach to investigate field-induced phenomena at surfaces. Very high electric field gradients are realized in an ultrahigh vacuum apparatus and tuned until controlled electron tunneling is triggered so as to produce interfacial redox chemical processes. The approach is exemplified in the case of a two-dimensional NiO/Ag(100)-(2x1) monolayer, and we demonstrate via STM and Auger experiments and theoretical modeling how reduction of the oxide phase to metallic Ni clusters can be selectively achieved via a dissociative electron attachment mechanism which has a resonant (threshold or activated) character and reaches an efficiency of several tens of a per cent.

Three points are worth noting. First, the present set-up is easily implemented and has general applicability, and can thus be used in a wide variety of contexts, from orienting the growth of ad-species on metal surfaces to promoting interfacial reactions and heterogeneous catalysis, thus promising to help elucidate several questions of interest in interface science. Phenomena such as sudden STM tip changes (as due to atom hopping onto/from the tip at biases exceeding a given threshold), electron beam manipulation[3,4], heterogeneous catalysis under an electric field[10], etc. are all

related to and can be clarified by the present work. Second, our results reconcile the discrepancy between the abundant theoretical predictions of field-induced effects[13,14,15,16,17,18,19,20] with the much rarer experimental realization [5,7,10] as due to the limitations of static modeling often used in the literature. Static modeling requires unrealistic field values to produce visible effects, but much before such high values are reached, competitive, current-based dynamic processes start being activated.[8,27,28] Third, the present approach can be seen as the area-averaged analogue of tip-promoted chemistry in STM experiments.[37,42,43,44,45,46,47] With respect to STM studies, the approach described here presents the attractive feature of the massive character of the associated chemical transformation that can be exploited in both research and technological applications,[50] e.g., in achieving the required efficiency in real-world energy storage devices.2 The crucial difference and novelty with respect to previous studies is that here we deal (i) not with single molecules but with a surface-science extended interfacial (multi-component) system, (ii) in which electrons are not provided by an external source but are generated in a rather controllable way by the field-induced current from the substrate and flow through the nanosized phase to drive a surface chemical reaction, in what may be called a "surface science electrochemistry" or "electrochemistry in vacuo" experiment.

Acknowledgements

This work has been supported by the ERC Advanced Grant SEPON. AF is grateful to Alessandro Lami and Erminald Bertel for very interesting discussions. Calculations were performed at CINECA within the ISCRA OAMONUA project.

Suppplementary Information

Details of theoretical modeling: computational details of the density-functional calculations, selected results of static DFT calculations including an electric field, definition of the electronic model Hamiltonian and plots of real orbitals involved in DEA, definition of the nuclear PES. Experimental additional information: typical Fowler-Nordheim I-V plot, estimate of experimental reduction efficiency, comparison of AES spectra obtained before and after electric-field exposure, induced NiO reduction by an inhomogeneous electric field, images of sputtered Ag(100) exposed to strong electric fields in the presence of an oxygen atmosphere and images of field-induced NiO reduction by an STM tip below -1.2 V. This material is available free of charge via the internet at http://pubs.acs.org.

Figure captions

Figure 1: Pictorial scheme of the experimental setup (**A**). Photograph of a miniature electrode (**B**).

Figure 2: Scanning tunneling microscopy images of NiO(2x1) nanostructures on Ag(100). As deposited (**A**), after annealing at 400 K (**B**), after annealing at 400 K in the presence of a spatially-extended homogeneous external DC-field (20 min at $\vec{E}$ = 1.5 V/nm) (**C**), after annealing the surface of (B) at 400 K in an oxygen partial pressure of $1x10^{-7}$ mbar at $\vec{E}$ = 2 V/nm for 20 min (**D**). Color code: Ag – yellow (top layer) and dark (second layer), NiO – green, Ni clusters – white. Imaging details: (**A**) -0.35 V, 700 pA, (**B**) 0.25 V, 700 pA, (**C**) 0.75 V, 600 pA, (**D**) 2V, 200 pA; all images are 50 x 50 nm^2 ; the initial NiO coverage was 0.7 ML in all cases.

Figure 3: Comparison of Auger electron spectra from NiO/Ag surface areas exposed to the electric field (I_F, red line) with non-exposed areas (I_0, black line). Both spectra are from the sample surface shown in Fig. 2d, the red line has been recorded approximately at the position of the STM image. The bottom panel displays the differences of the two spectra [$(I_0-I_F)/max(I_0)$; dots – point-by-point ratio, red line – moving-window average (8 points)]. Detailed spectra of the oxygen KLL Auger region are shown in the inset; the full lines are moving-window averages (5 points).

Figure 4: Schematic depiction of the experimental situation (**A**). Structural model of a section of the NiO/Ag(100)-(2x1) phase (left) and its 1D analogue (right) (**B**). 1D idealized system on which the DEA matrix element is calculated (left) and electronic spectrum of the corresponding Dirac-delta-function potential molecule (right) (**C**).

Figure 5: Potential energy surfaces (PES) used to calculate the nuclear wave functions: $PES_i(R)$ for the initial state neutral AB molecule and $PES_f(R)$ for the final state AB^- negative ion (**A**). Total cross-section of the DEA process evaluated as in Eq. (2) as a function of the nuclear energy $\eta = K^2/2$ in the outgoing continuum. All energies in eV, *R* in a.u. (**B**)

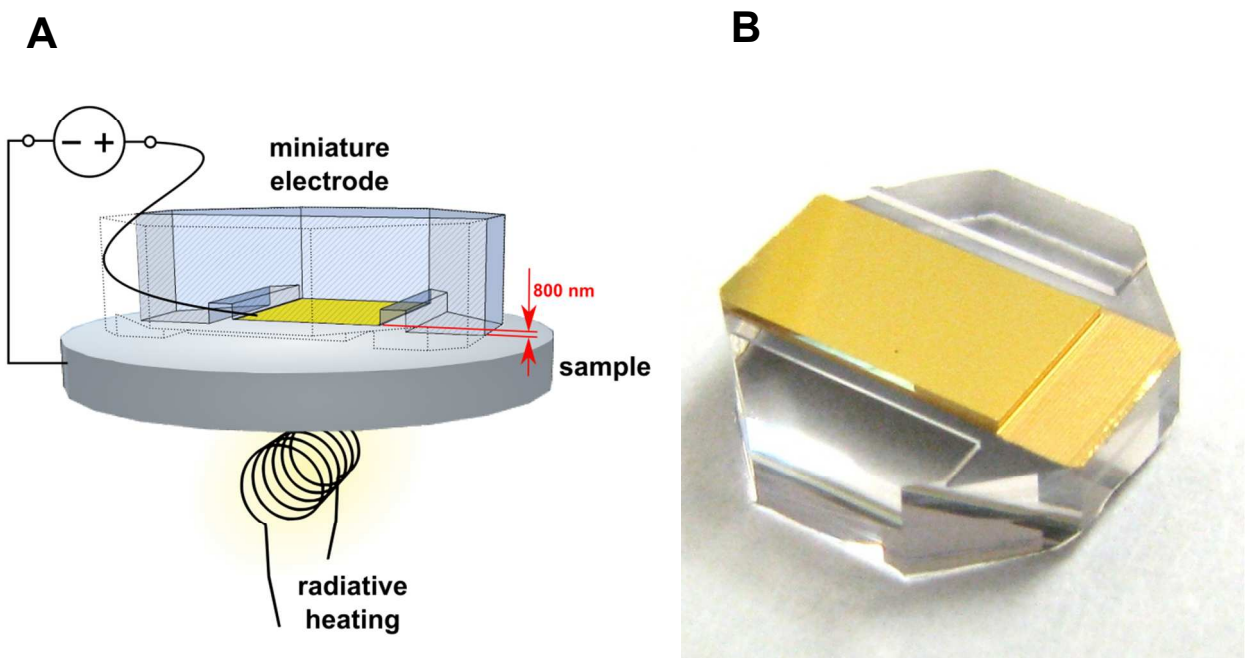

Figure 1

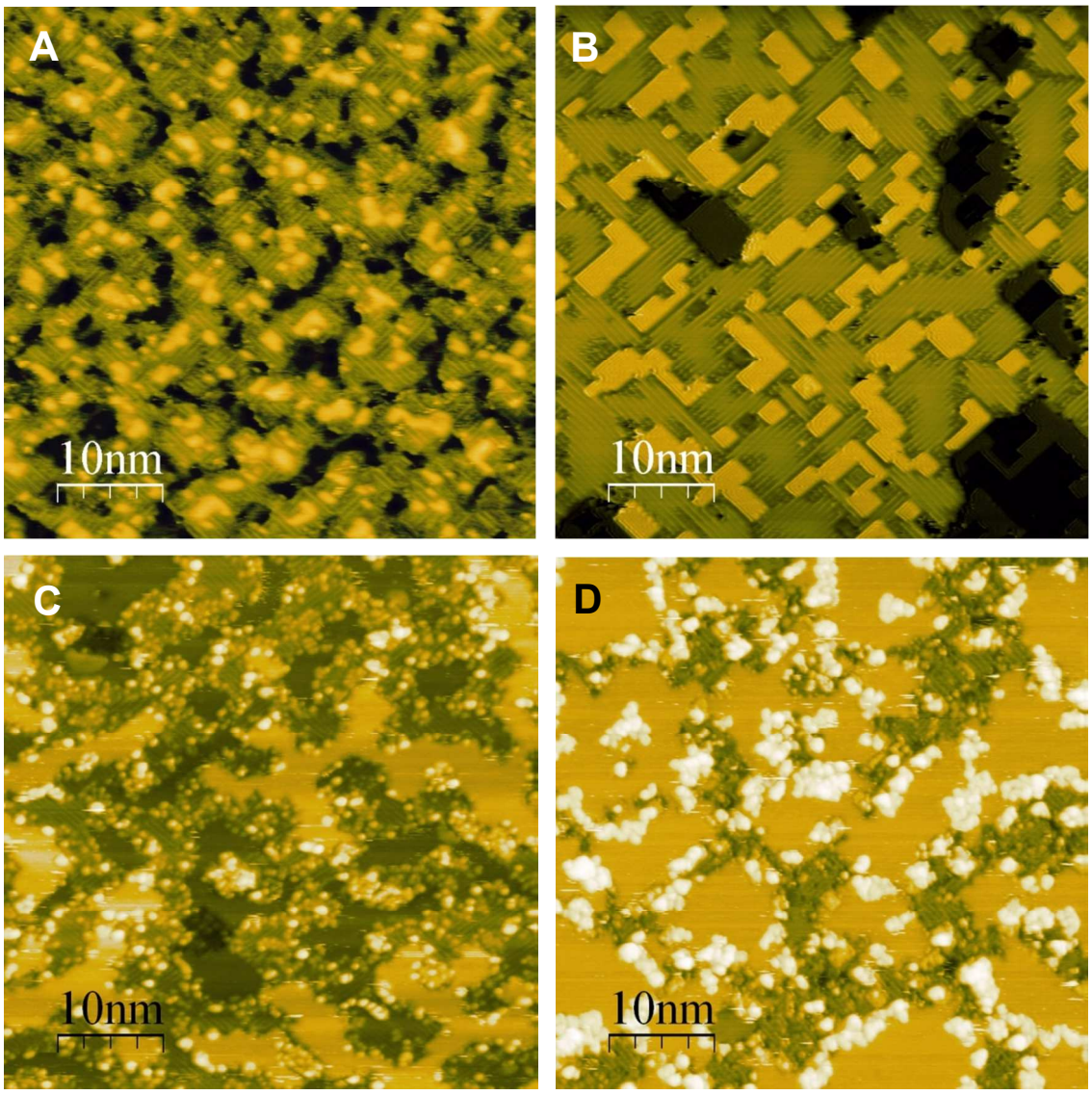

Figure 2

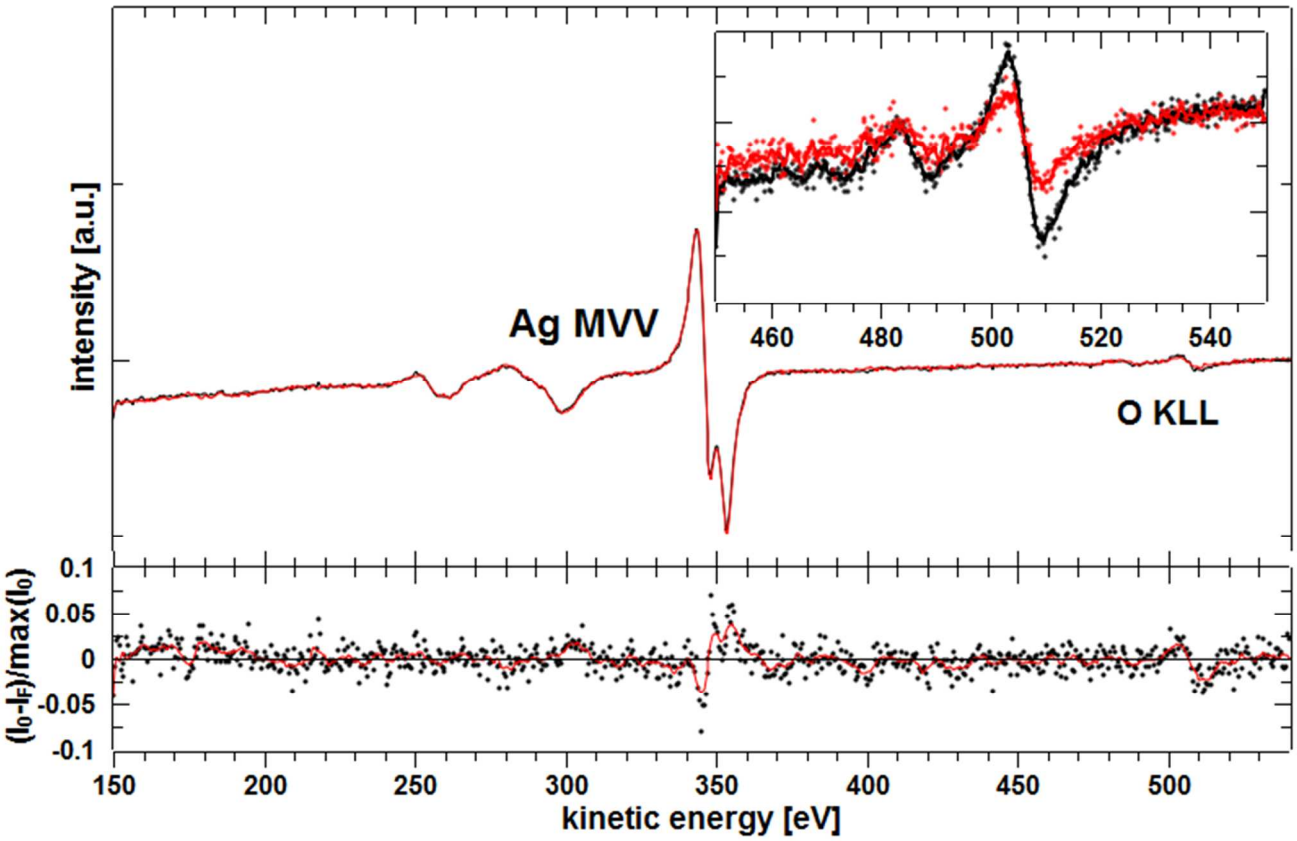
intensity [a.u.]
Ag MVV
O KLL
460
480
500
520
540
0.1
0.05
0
-0.05
-0.1
(I0-IF)/max(I0)
150
200
250
300
350
400
450
500
kinetic energy [eV]

Figure 3

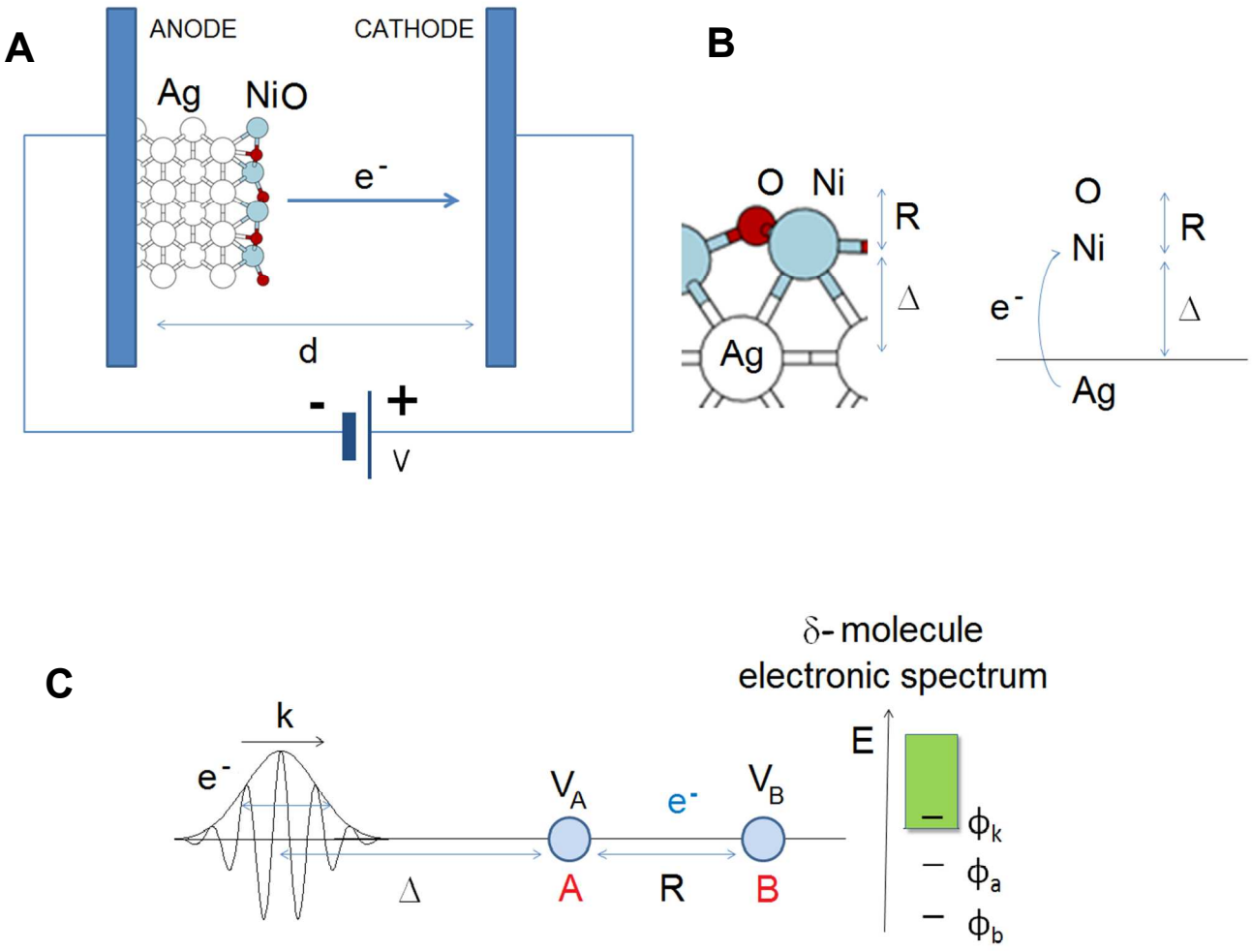
A
ANODE
CATHODE
Ag
NiO
e-
d
-
+
V
B
O
Ni
R
Δ
Ag
O
Ni
R
e-
Δ
Ag
C
δ- molecule
electronic spectrum
k
e-
Δ
VA
A
e-
R
VB
B
E
ϕk
ϕa
ϕb

Figure 4

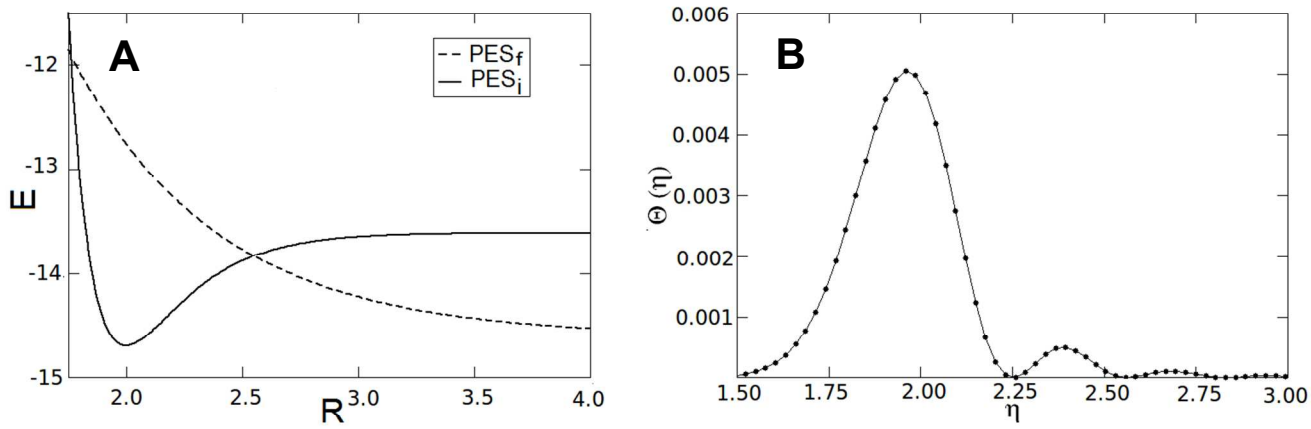
A
PES$_f$
PES$_i$
E
R
-12
-13
-14
-15
2.0
2.5
3.0
3.5
4.0
B
Θ (η)
η
0.006
0.005
0.004
0.003
0.002
0.001
1.50
1.75
2.00
2.25
2.50
2.75
3.00

Figure 5

References

[1] R. A. Marcus, *Rev. Mod. Phys.* **65**, 599 (1993).

[2] N. S. Lewis, D. G. Nocera, *PNAS* **103**, 15729 (2006).

[3] L. G. Christophorou, E. Illenberger, and W. F. Schmidt, *Linking the Gaseous and the Condensed Phases of Matter: The Slow Electron and Its Interactions* (Plenum, New York, 1994).

[4] C. R. Arumainayagam, H.-L. Lee, R. B. Nelson, D. R. Haines, R. P. Gunawardane, *Surf. Sci. Rep.* **65**, 1 (2010).

[5] J. Jeong, N. Aetukuri, T. Graf, T. D. Schladt, M. G. Samant, S. S. P. Parkin, *Science* **339**, 1402 (2013).

[6] T. Maruyama, Y. Shiota, T. Nozaki, K. Ohta, N. Toda, M. Mizuguchi, A. A. Tulapurkar, T. Shinjo, M. Shiraishi, S. Mizukami, Y. Ando, Y. Suzuki, *Nat. Nanotech.* **4**, 158 (2009).

[7] H. Dai, *Acc. Chem. Res.* **35**, 1035 (2002).

[8] V. Gill, P. Guduru, and B. Sheldon, *Int. J. Solids Struct.* **45**, 943 (2008).

[9] H. Liu, C. Song, L. Zhang, J. Zhang, H. Wang, D. P. Wilkinson, *J. Power Sources* **155**, 95 (2006).

[10] T. Visart de Bocarmé, N. Kruse, *Ultramicroscopy* **111**, 376 (2011).

[11] W. Steurer, F. Allegretti, S. Surnev, G. Barcaro, L. Sementa, F. Negreiros, A. Fortunelli, F. P. Netzer, *Phys. Rev. B* **84**, 115446 (2011).

[12] S. Surnev, A. Fortunelli, F. P. Netzer, *Chem. Rev.* **113**, 4314-4372 (2013).

[13] B. Yoon and U. Landman, *Phys. Rev. Lett.* **100**, 56102 (2008).

[14] R. Gu, Z. Wang, and C. Ting, *Phys. Rev. B* **67**, 153101 (2003).

[15] N. N. Negulyaev, V. S. Stepanyuk, W. Hergert, and J. Kirschner, *Phys. Rev. Lett.* **106**, 037202 (2011).

[16] J. Zhou and Q. Williams, *J. Phys.: Cond. Matter* **21**, 055008 (2009).

[17] J. Burton, E. Tsymbal, *Phys. Rev. B* **80**, 174406 (2009).

[18] Y. He, X. Y. Wei, C. T. Chan, and J. G. Che, *Phys. Rev. B* **71**, 045401 (2005).

[19] M. Tsujikawa, T. Oda, *Phys. Rev. Lett.* **102**, 247203 (2009).

[20] B. Jeon, Q. Van Overmeere, A. C. T. Van Duinc and S. Ramanathan, *Phys. Chem. Chem. Phys.* **15**, 1821 (2013).

[21] W. Steurer, S. Surnev, F. Hanauer, K. Ansperger, and F. Netzer, *A setup for the study of surface processes under spatially-extended homogeneous external electric fields >2 V/nm* (2013) (unpublished), see http://arxiv.org/abs/1311.5356.

[22] M. Caffio, A. Atrei, U. Bardi, and G. Rovida, *Surface Science* **588**, 135 (2005).

[23] As the sample is transferred between the individual stages (sputtering, E-field, STM) several times per day, contamination of the single-crystal surface with small particles cannot be prevented completely. Ar+ sputtering, which is the only method to clean the Ag(100) crystal surface in UHV, is very inefficient for removing particles. For example, hundreds of sputter cycles are required to completely remove a particle that is 300 nm in size.

[24] R. G. Forbes, J. H. B. Deane, N. Hamid, H. San Sim, *J. Vac. Sci. Technol. B* **22**, 1342 (2004).

[25] see *Supplementary Information*. Details of theoretical modeling: computational details of the density-functional calculations, selected results of static DFT calculations including an electric field, definition of the electronic model Hamiltonian and plots of real orbitals involved in DEA, definition of the nuclear PES. Experimental additional information: typical Fowler-Nordheim I-V plot, estimate of experimental reduction efficiency, comparison of AES spectra obtained before and after electric-field exposure, induced NiO reduction by an inhomogeneous electric field, images of sputtered Ag(100) exposed to strong electric fields in the presence of an oxygen atmosphere and images of field-induced NiO reduction by an STM tip below -1.2 V.

[26] In the present case we found from density-functional theory calculations (see the Supplementary Information, SI, for technical details) that only fields of the order of at least 50 V/nm do produce an appreciable change in the charge distribution and energetics of the NiO/Ag(100)-(2x1) phase. In the SI more precise estimates are provided.

[27] N. M. Caffrey, T. Archer, I. Rungger, S. Sanvito, *Phys. Rev. Lett.* **109**, 226803 (2012).

[28] Y. Zhang, C. Y. Yam, G.H. Chen, *J. Chem. Phys.* **138**, 164121 (2013).

[29] T. F. O'Malley, *Phys. Rev.* **150**, 14 (1966).

[30] W. Domcke, *Phys. Rep.* **208**, 97 (1991).

[31] Note that at such relatively low fluxes (less than 1 electron/μsec/surface-atom even assuming the strictest estimate of conducting area – see below) current-induced ionic heating can be neglected, see e.g. M. Di Ventra "Electrical Transport in Nanoscale Systems" Cambridge University Press, Cambridge (UK), 2008.

[32] R. E. Palmer, *Progr. Surf. Sci.* **41**, 51 (1992).

[33] J. M. White *J. Mol. Cat. A* **131**, 71 (1998).

[34] I. Bald, J. Langer, P. Tegeder, O. Ingólfsson, *Int. J. Mass Spectrom.* **277**, 4 (2008).

[35] M. Braun, M.-W. Ruf, I. I. Fabrikant, H. Hotop, ICAMDATA-2008, *AIP Conference Proceedings* **1125**, 39 (2009).

[36] J. W. Gadzuk, *J. Chem. Phys.* **137**, 091703 (2012).

[37] T. Ohto, I. Rungger, K. Yamashita, H. Nakamura, S. Sanvito, *Phys. Rev. B* **87**, 205439 (2013).

[38] H. Hogreve, *Int. J. Quantum Chem.* **109**, 1430 (2009).

[39] J. C. Tully, *J. Chem. Phys.* **93**, 1061 (1990).

[40] Note that to simplify the asymptotic boundary conditions in the nuclear calculations and be able to define a value of the nuclear momentum (K), we have considered the effect of the electric field in deforming the PES around the equilibrium geometry but not at the asymptotes: this should not change qualitatively the results as the cross section matrix element is concentrated in the region of the maximum of the ground-state nuclear wave function.

[41] B. C. Stipe, M. A. Rezaei, W. Ho, S. Gao, M. Persson, B. I. Lundqvist, *Phys. Rev. Lett.* **78**, 4410 (1997).

[42] Y. Xie, C. Bell, T. Yajima, Y. Hikita, and H. Hwang, *Nano Lett.* **10**, 2588 (2010).

[43] N. Jiang, Y. Zhang, Q. Liu, Z. Cheng, Z. Deng, S. Du, H. Gao, M. Beck, and S. Pantelides, *Nano Lett.* **10**, 1184 (2010).

[44] M. Alemani, M. V. Peters, S. Hecht, K.-H. Rieder, F. Moresco, and L. Grill, *J. Am. Chem. Soc.* **128**, 14446 (2006).

[45] S. Gwo, C.-L. Yeh, P.-F. Chen, Y.-C. Chou, T. T. Chen, T.-S. Chao, S.-F. Hu, and T.-Y. Huang, *Appl. Phys. Lett.* **74**, 1090 (1999).

[46] A. A. Shklyaev, M. Shibata, and M. Ichikawa*, J. Appl. Phys.* **88**, 1397 (2000).

[47] S. Maier, I. Stass, J. I. Cerda, M. Salmeron, *J. Phys. Chem. C* **116** , 25395 (2012).

[48] Y. W. Mo, *Phys. Rev. Lett.* **71**, 2923 (1993).

[49] The electron affinity of Mn is appreciably lower that that of Ni – see e.g. Handbook of Chemistry and Physics, edited by D. R. Lide, 72th ed., CRC, Boca Raton, (1991) – and the fact that the MnO phase is more embedded than the NiO phase also contributes to favoring Ag diffusion.

[50] N. J. Mason, *Int. J. Mass Spectrom.* **277**, 31 (2008).